

# Variations in protein expression associated with oral cancer

Wei Jiang<sup>a,d,1</sup>, Zhiyan He<sup>a,c,1</sup>, Youmeng Zhang<sup>b,1</sup>, Shujun Ran<sup>a</sup>, Zhe Sun<sup>a,\*</sup> and Weixu Chen<sup>b,\*</sup>

<sup>a</sup>*Department of Endodontics and Operative Dentistry, Shanghai Ninth People's Hospital, Shanghai Jiaotong University School of Medicine, College of Stomatology, National Clinical Research Center for Oral Diseases, Shanghai Key Laboratory of Stomatology, Shanghai, China*

<sup>b</sup>*Department of Stomatology, Eye & Ent Hospital of Fudan University, Shanghai, China*

<sup>c</sup>*Shanghai Research Institute of Stomatology, Ninth People's Hospital, School of Medicine, Shanghai Jiao Tong University, Shanghai, China*

<sup>d</sup>*Department of Stomatology, Shanghai Hudong Hospital, Shanghai, China*

## Abstract.

**BACKGROUND:** Differential protein expression of the oral microbiome is related to human diseases, including cancer.

**OBJECTIVE:** In order to reveal the potential relationship between oral bacterial protein expression in oral squamous cell carcinoma (OSCC), we designed this study.

**METHODS:** We obtained samples of the same patient from cancer lesion and anatomically matched normal site. Then, we used the label free quantitative technique based on liquid chromatography tandem mass spectrometry (LC-MS/MS) to analyze the bacteria in the samples of oral squamous cell carcinoma at the protein level, so as to detect the functional proteins.

**RESULTS:** Protein diversity in the cancer samples was significantly greater than in the normal samples. We identified a substantially higher number of the taxa than those detected in previous studies, demonstrating the presence of a remarkable number of proteins in the groups. In particular, proteins involved in energy production and conversion, proton transport, hydrogen transport and hydrogen ion transmembrane transport, ATP-binding cassette (ABC) transporter, PTS system, and L-serine dehydratase were enriched significantly in the experimental group. Moreover, some proteins associated with Actinomyces and Fusobacterium were highly associated with OSCC and provided a good diagnostic outcome.

**CONCLUSION:** The present study revealed considerable changes in the expression of bacterial proteins in OSCC and enrich our understanding in this point.

Keywords: OSCC, LC-MS/MS, protein expression, energy production, proton transport

## 1. Introduction

Oral cancer is the sixth most common malignant tumor in the world. Oral squamous cell carcinoma (OSCC) accounts for more than 90% of oral cancer cases. OSCC originates from oral mucosal epithelium

<sup>1</sup>These authors contributed equally to the work and should be considered co-first authors.

\*Corresponding authors: Weixu Chen, Department of Stomatology, Eye and Ent Hospital of Fudan University; No. 39 Baoqing Road, Shanghai, China. E-mail: Chenweixu9999@163.com; Zhe Sun, Department of Endodontics and Operative Dentistry, Shanghai Ninth People's Hospital, Shanghai Jiaotong University School of Medicine, College of Stomatology, National Clinical Research Center for Oral Diseases, Shanghai Key Laboratory of Stomatology, No. 639 Zhizaoju Road, Shanghai, China. E-mail: sunzhe3272@163.com.

and is the most common malignant tumor of the head and neck. Approximately 300,000 new cases of OSCC are diagnosed every year [1]. Patients with early- and middle-stage oral squamous cell carcinoma are usually treated surgically. For patients with multiple positive lymph nodes or metastasis, this treatment is usually supplemented with postoperative radiotherapy and chemotherapy. The 5-year survival rate of patients with OSCC is less than 60% [2]. Generally, smoking and alcoholism are considered the main risk factors for OSCC. HPV infection, poor oral hygiene, long-term chronic stimulation and other factors are also related to the occurrence and development [3]. Candida infection is also considered a predisposing factor of OSCC. However, whether other bacteria and microorganisms and proteins they secrete are involved in the occurrence, development, and prognostic assessment of OSCC is not been fully studied. Recent relevant studies have shown that bacteria or microorganisms may be involved in the occurrence of cancer [4].

Most of the cellular activities occur at the protein level, and small changes in protein expression have a great impact on vital activities and operation of the organisms. Surface proteins are important proteins, which contact with external environment directly. These proteins are closely related to environmental adaptability, pathogenicity, and drug resistance of bacteria. Secretory proteins are released by the cells to mediate interactions between a pathogen and the host.

So far, some changes in protein variation have been related to several types of cancer [5]. Some early studies using molecular techniques evaluated changes in cancer-related protein expression [6–11]; However, due to the limited number of strains/clones that can be tested, no consensus has been reached.

In the postgenomic era, the emergence of label-free quantitative technology based on liquid chromatography-tandem mass spectrometry (label-free LC-MS/MS) enables accurate comparative analysis of all proteins expressed by the cells under various physiological and pathological conditions. Quantification and identification of these proteins will help us to find biomolecules directly related to specific physiological or pathological states. The emergence of LS/MS enables profiling of microbial communities at an unprecedented depth and coverage. This technology can be used to determine what changes in the surface and secretory proteins are present in OSCC versus normal mucosa.

Some studies have employed LS/MS to assess protein expression in OSCC. Pushalkar et al. [12] studied relative abundance and the diversity of proteins in the saliva of subjects with OSCC; however, only three OSCC cases and two healthy controls were included. Another paper evaluated salivary bacterial communities in six OSCC patients by pyrosequencing, and paired taxa within the Enterobacteriaceae family together with the *Oribacterium* genus, which were suggested to distinguish OSCC samples from the subjects with oropharyngeal squamous cell carcinoma (OPSCC) and normal ones [13]. These studies failed to analyze all the differences in the protein composition in healthy versus diseased mucosa, even though specific proteins are sometimes involved in a disease. Al-hebshi successfully profiled bacterial communities in 23 OSCC tissue samples from Yemeni patients at the species level, this is the first epidemiological evidence for associations of *Fusobacterium nucleatum* and *Pseudomonas aeruginosa* with OSCC [14,15]. But because the number of OSCC patients included is too limited, it is hard to make sure the significance of the findings. Additional studies to validate these results are needed. In the present study, the samples of cancer lesions and matched controls were acquired from 30 Chinese subjects with OSCC. Protein profiles of the samples were characterized. We analyzed the changes in protein composition and functions associated with OSCC. Moreover, a group of periodontitis-related bacteria that was significantly enriched in OSCC samples were found in our study. Our findings may contribute to further clarification of a connection between OSCC and protein expression.

We hypothesized that the changes in oral bacterial protein expression were correlated with the occurrence, development, and prognosis of oral squamous cell carcinoma; oral bacterial infection may

directly or indirectly cause epigenetic variations in the genes of regional epithelial cells through chronic inflammation or along with other stimulating factors (smoking, alcoholism, chronic stimulation, etc.) thus participating in the reconstruction of the tumor microenvironment.

## 2. Materials and methods

### 2.1. Subject recruitment and sample collection

Thirty OSCC patients (15 males and 15 females) in the early stage with a mean age of 55 were recruited from the Department of Oral and Maxillofacial-Head and Neck Oncology of the Ninth People's Hospital (Shanghai, China). The patients did not have detectable periodontal inflammation, oral mucosal diseases, visible carious lesions, or any severe systemic disorders (such as immune compromise, diabetes, or genetic diseases). Furthermore, the patients had not taken antibiotics or received treatment for OSCC at least two weeks prior to the sampling and consented to clinical examination and sampling. The present study was approved by the Ethics Committee of Shanghai Ninth People's Hospital affiliated with the Shanghai Jiao Tong University School of Medicine. Written informed consent was obtained from all subjects. All experiments were performed according to approved guidelines.

The swabs of oral lesions and anatomically matched normal sites were collected according to a well-defined clinical protocol [13]. Subjects were prevented from drinking and eating for at least 2 h before the sampling. All samples were transported to the laboratory on ice within 2 h of collection and were stored at  $-80^{\circ}\text{C}$  before subsequent processing.

### 2.2. Sample preparation

Use liquid nitrogen to grind the sample into powder in mortar. Quickly transfer all powder samples to 1.5 ml centrifuge tubes precooled in liquid nitrogen, and add 200 to each tube  $\mu\text{L}$  SDT protein cleavage buffer (4% SDS, 100 mM Tris HCl and 100 mM dithiothreitol (DTT), pH 8.0); The samples were placed in a boiling water bath for 10 minutes, sonicated in an ice bath for 10 minutes (every 7 seconds, 40 W, 3 seconds), placed in a boiling water bath for 5 minutes, and centrifuged at 14000 g for 30 minutes. Collect the supernatant and pass 0.22  $\mu\text{M}$  ultrafiltration tube filtration. The filtrate is stored at  $-80^{\circ}\text{C}$ .

After thawing the samples at  $4^{\circ}\text{C}$ , 10  $\mu\text{L}$  of the samples were supplemented with 2  $\mu\text{L}$  of  $5\times$  loading buffer (250 mM Tris-HCl (pH 6.8), 10% (w/v) SDS, 0.5% (w/v) BPB, 50% (v/v) glycerin, and 5% DTT), mixed, and heated at  $98^{\circ}\text{C}$  for 3 min; the samples were cooled to room temperature, centrifuged at 3,000 g for 1 min, and loaded to perform electrophoresis (100 V for 10 min and 200 V for 30 min). After electrophoresis, the gel was slightly washed with deionized water to remove electrophoresis buffer. Then, the gels were quickly silver-stained. The images were scanned and recorded. The samples were finally investigated by screening of the images.

### 2.3. Protein extraction and peptide sample preparation for mass spectrometry

100 per sample in total  $\mu\text{L}$  for FASP digestion; Add 100 mM DTT to the sample, boil it in water for 5 minutes and cool it to room temperature. Add and mix total 200  $\mu\text{L}$  UA buffer (8 M urea and 150 mM Tris HCl, pH 8.5) and transfer the solution to a 30 kDa ultrafiltration tube; The sample was centrifuged at 14000 g for 30 minutes at room temperature; Discard the filtrate and repeat the above steps 3 times. Add 100 in total  $\mu\text{L}$  IAA (50 mM IAA in UA); The samples were shaken at 600 rpm for 1 minute, incubated in

the dark at 300 rpm at room temperature for 30 minutes, and centrifuged at 14000 g at room temperature for 30 minutes. Add total 100  $\mu\text{L}$  UA buffer, and centrifuge the sample at 14000 g for 30 minutes at room temperature; These steps were repeated three times. Add 100 in total  $\mu\text{L}$  25 mM ABC buffer and centrifuge the sample at 14000 g for 30 minutes at room temperature; These steps are repeated four times. Finally, discard the filtrate and add 40  $\mu\text{L}$  trypsin buffer (at 40  $\mu\text{L}$  Add 2 to 1 100 mM ABC buffer  $\mu\text{g}$  trypsin) and place the mixture on a thermostatic mixer (300 rpm, 18 h, 37°C). Collect the filtrate by centrifuging at 14000 g for 30 minutes at room temperature; Replace the collecting pipe and add 40  $\mu\text{L}$  25 mM ABC buffer; The sample was centrifuged at 14000 g for 30 minutes at room temperature to obtain the filtrate, and the peptide was quantified using OD 280.

#### 2.4. Liquid chromatography-tandem mass spectrometry analysis

Solvent A is an aqueous solution of 0.1% formic acid, and solvent B is a solution of 0.1% formic acid in 100% acetonitrile. Use 95% solvent A to balance the thermal scientific analysis column (75  $\mu\text{m}$   $\times$  25 cm, 5  $\mu\text{m}$ , 100 Å, C18). Use the autosampler to load the sample into the thermosience easy catch column (100  $\mu\text{m}$   $\times$  2 cm, 5  $\mu\text{m}$ , 100 Å, C18), and then separated by chromatographic column. The relevant liquid phase gradient is as follows: 0–132 minutes, the linear gradient of solvent B ranges from 3% to 24%; 132–200 minutes, the linear gradient of liquid solvent B ranges from 24% to 42%; In 200–235 minutes, the linear gradient of liquid solvent B ranges from 42% to 90%; 90% solvent B is maintained at 235–240 minutes. The enzymolysis products were desalted, separated by capillary high performance liquid chromatography, and analyzed by tandem mass spectrometry using a q-exactive mass spectrometer (thermo Finnigan, San Jose, California). Analysis time: 240 minutes. Detection method: positive ion. Scanning range of parent ion: 350–2000 m/z. Resolution of primary mass spectrometry: 70000@m/z 200. AGC target: 3e6. Level 1 maximum it: 50 ms. Number of scanning ranges: 1. Dynamic exclusion: 30.0S. The mass charge ratio of peptides and peptide fragments was obtained according to the following methods: 20 fragment maps were obtained after each full scan (MS2 scan); MS2 activation type: HCD; Isolation window: 1.2; Resolution of secondary mass spectrometry: 17500@m/z 200; MICROSCAN: 1; Secondary maximum it: 100 ms; AGC target: 1E5; Normalized collision energy: 32 EV; Underfill rate: 2%.

#### 2.5. Database creation and searching for identification and quantification of the peptides and proteins

To increase the sensitivity of a large data search, the MetaPro-IQ approach was used to identify and quantify the peptides and proteins using the raw data of mass spectrometry. Briefly, the whole oral microbiome gene catalog database was initially downloaded from the Human Oral Microbiome Database (HOME, version: 9.0, <http://www.homd.org>). Then, Proteome Discoverer (version 2.1) was used to search against this database to generate a “pseudometaproteome” database for each sample. A reduced database containing all possible proteins derived from the peptide spectrum matches was generated and hyphenated using reversed sequences for each sample for a typical target-decoy database search. FDR < 0.01 filtering was used to confidently confirm the lists of identified peptides and proteins. The final protein database was created by combining and deduplicating all resulting protein lists. Finally, all raw files were imported into MaxQuant (version: 1.6.5.0) for peptide and protein identification and quantification based on this database. Search parameters of Maxquant for the protein database were as follows: trypsin, two maximum missed cleavages; oxidation (methionine) and acetyl (protein N-terminus) as variable modifications; carbamidomethylation (cysteine) as fixed modification; LFQ and iBAQ label-free quantification; 6 ppm for main search; revert decoy mode; PSM FDR 0.01; protein FDR 0.01; 2 minimal peptide length; unique + razor peptides for quantification; 20 ppm FTMS MS/MS tolerance; and 12 FTMS top peaks per 100 Da.

## 2.6. Microbial taxonomic analysis

All peptide sequences identified by MaxQuant were submitted to the ‘Metaproteome analysis’ module of the UniPept web application (version: 4.2) for microbial taxonomic analysis with the “Equate I and L” and “Advanced missing cleavage handling” options. Moreover, all identified top rank proteins were assigned to the corresponding taxa by an in-house Perl script based on the taxonomic level file obtained from the HOMD. Unmatched top proteins were manually searched using the Taxonomy database of the NCBI by keywords (genus name) in protein description. Statistics and plots of taxonomic analysis were assessed by R (version: 3.5.1, <https://www.r-project.org/>). The Krona charts of identified bacteria were created by the Krona Excel template based on protein counts and LFQ intensity accumulation (Krona Excel template: <https://github.com/marbl/Krona/wiki/ExcelTemplate>).

At all taxa levels, the Mann-Whitney U test and paired sample t test were used to identify differentially abundant taxa in the two groups based on log<sub>10</sub>-transformed cumulative LFQ intensity calculated using R.

## 2.7. Microbial function and pathway analysis

A standalone BLASTP(version:2.2.31+) was used to match all identified microbial proteins to the UniProtKB/Swiss-Prot database, which included 560,118 sequences, and the COG database (version: 2014), which included 1,781,653 sequences for obtaining function annotations. Furthermore, gene ontology (GO) functional annotations were predicted by InterProScan (version: 5.35–74.0) with default parameters. Moreover, KEGG Orthology Based Annotation System (KOBAS version:3.0), parameters: E-value≤1e-05, rank≤5) was performed for the KEGG Orthology (KO) annotation prediction and binomial tests were performed between the B and Z groups at the KEGG pathway level. Then, the KronaTools was used to plot the Krona chart for visualizing assignment of the proteins at the KEGG pathway level. Besides, statistical analysis and graphics drawing were completed with R (version:3.6.3).

## 2.8. Statistical and multivariate data analysis

We used the equation  $\log_{10}(\text{LFQ intensity} + 1)$  to transform the LFQ intensity of quantified protein groups in R for subsequent statistical analysis. After removing the proteins that lacked LFQ signals in all samples, univariate significant differences between the B and Z groups were assessed by the paired sample T test using R (version: 3.5.1). Moreover, after imputing missing values as one thousandth of the minimum value, partial least squares discriminant analysis (PLS-DA) was performed to assess differentially expressed proteins using the MetaboAnalystR package. Only those protein groups with valid LFQ intensity values in  $\geq 50\%$  of the samples were used for multivariate statistical analysis. Principal component analysis (PCA) and PLS-DA were performed by the mixOmics package. Hierarchical clustering analysis and heatmap plotting were performed by the R pheatmap package.

## 2.9. Verification with parallel reaction monitoring technology

The appropriated target peptides were selected by analyzing the results of the original label-free-based quantitative. Then, these peptides were performed targeted shotgun MS to select peptides for PRM quantification analysis. Finally, the Xcalibur software was used to implement Parallel Reaction Monitoring (PRM) analysis of target peptides.

Statistical analysis was performed by R and the ‘MetaboAnalystR’ package.

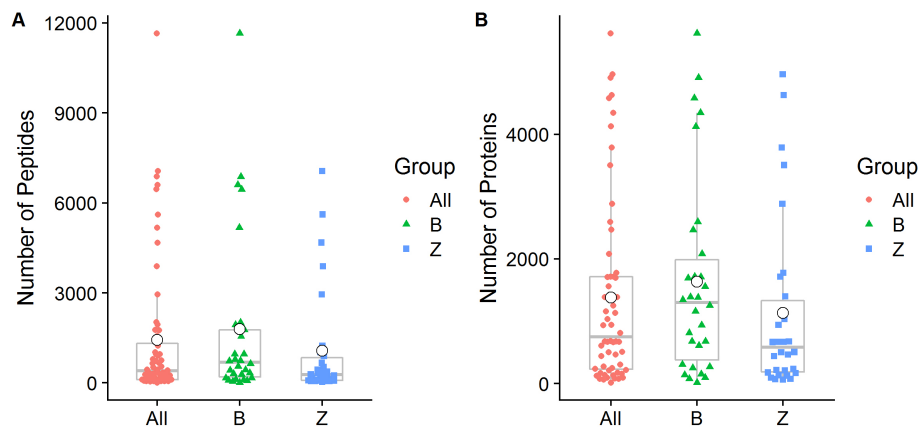


Fig. 1. Peptide and protein group identification by oral metaproteomics. (A) Box plot representations of the number of peptides identified in the present study. (B) Box plot representations of the number of identified proteins. Different colors of the symbols are used to represent individual samples, and the median (central lines), mean (white small dot), 25% and 75% quartile ranges (box width), and upper and lower limits (asterisk) are shown. All: All samples from 30 OSCC patients; B: Swabs of lesion surfaces; Z: Contralateral normal mucosa.

### 2.10. Data availability

All MS raw files were submitted to the ProteomeXchange Consortium (<http://www.proteomexchange.com>) via the PRIDE partner repository with the dataset identifier.

## 3. Results

### 3.1. Statistics of the number of identified peptide sequences and protein groups

We quantified a total of 38,536 peptide sequences and 11,469 protein groups that covered at least one peptide in 60 samples of 30 OSCC patients. A total of 26,389 (68.48%) of these peptide sequences were confirmed as unique peptides. On average,  $1,428 \pm 304$  peptide sequences and  $1,382 \pm 194$  protein groups were identified per sample. In addition, a mean of  $1,790 \pm 503$  peptide sequences and  $1,632 \pm 289$  protein groups were identified per sample of Group B (swabs of lesion surfaces). As expected,  $1,066 \pm 336$  mean peptide sequences and  $1,131 \pm 256$  protein groups for Group Z (contralateral normal mucosa) were slightly lower than the counts detected in Group B (Fig. 1). Using the ‘Stats’ package of R,  $p = 0.009108$  and  $p$  value = 0.03148 was computed based on the paired sample T test of the B versus Z groups. The  $p$  values indicated that the peptide and protein counts of Group B were significantly greater than those of Group Z. A total of 10,773 nonredundant protein groups were identified in Group B samples, and 7,855 nonredundant protein groups were identified in Group Z samples and had 7,159 shared proteins between the two groups.

### 3.2. Taxonomic analysis of the microbiome by metaproteomics

Taxonomic characterization is important in microbiome studies. In the present study, we attempted to use two strategies to explore the taxonomic composition of the microbiome. According to the first strategy, all 38,536 identified peptide sequences were submitted to UniPept (version: 4.2) to perform



Table 1  
Significantly different taxa

Level	Taxa	<i>p</i> value according to the paired-sample T test
Phylum	Synergistetes	0.0128
Phylum	Spirochaetes	0.0353
Class	Flavobacteriia	0.0039
Class	Epsilonproteobacteria	0.0082
Class	Spirochaetia	0.0353
Order	Flavobacteriales	0.0039
Order	Pasteurellales	0.0048
Order	Campylobacteriales	0.0082
Order	Spirochaetales	0.0353
Order	Xanthomonadales	0.0438
Order	Coriobacteriales	0.0450
Family	Flavobacteriaceae	0.0039
Family	Pasteurellaceae	0.0048
Family	Lactobacillaceae	0.0246
Family	Brucellaceae	0.0257
Family	Campylobacteraceae	0.0289
Family	Coriobacteriaceae	0.0328
Family	Spirochaetaceae	0.0353
Family	Xanthomonadaceae	0.0438
Family	Enterococcaceae	0.0469
Family	Bradyrhizobiaceae	0.0498
Family	Eubacteriaceae [XV]	0.0681
Genus	Capnocytophaga	0.0039
Genus	Haemophilus	0.0119
Genus	Candidate	0.0164
Genus	Lactobacillus	0.0246
Genus	Corynebacterium	0.0256
Genus	Ochrobactrum	0.0257
Genus	Campylobacter	0.0289
Genus	Treponema	0.0353
Genus	Eikenella	0.0407
Genus	Stenotrophomonas	0.0438
Genus	Peptostreptococcea [13][G-1]	0.0438
Genus	Enterococcus	0.0469
Species	Haemophilus parainfluenzae	0.0011
Species	Capnocytophaga sputigena	0.0054
Species	Fusobacterium sp.	0.0065
Species	Neisseria subflava	0.0140
Species	Haemophilus sp.	0.0141
Species	Prevotella intermedia	0.0149
Species	Prevotella sp.	0.0151
Species	Aggregatibacter actinomycetemcomitans	0.0151
Species	Neisseria mucosa	0.0152
Species	Candidate division	0.0164
Species	Capnocytophaga sp.	0.0188
Species	Aggregatibacter sp.	0.0189
Species	Treponema medium	0.0197
Species	Streptococcus anginosus	0.0209
Species	Capnocytophaga gingivalis	0.0210
Species	Haemophilus influenzae	0.0212
Species	Propionibacterium sp.	0.0212
Species	Selenomonas noxia	0.0215
Species	Neisseria flavescens	0.0223

Table 1, continued

Level	Taxa	<i>p</i> value according to the paired-sample T test
Species	Tannerella forsythia	0.0232
Species	Ochrobactrum anthropi	0.0257
Species	Cardiobacterium valvarum	0.0264
Species	Leptotrichia shahii	0.0264
Species	Kingella denitrificans	0.0306
Species	Campylobacter concisus	0.0326
Species	Eikenella corrodens	0.0407
Species	Prevotella salivae	0.0412
Species	Selenomonas artemidis	0.0437
Species	Stenotrophomonas maltophilia	0.0438
Species	Peptostreptococcacea (13)[G-1] sp.	0.0438
Species	Neisseria bacilliformis	0.0450
Species	Prevotella marshii	0.0466
Species	Fusobacterium periodonticum	0.0479
Species	Selenomonas flueggei	0.0549

T: paired sample T test.

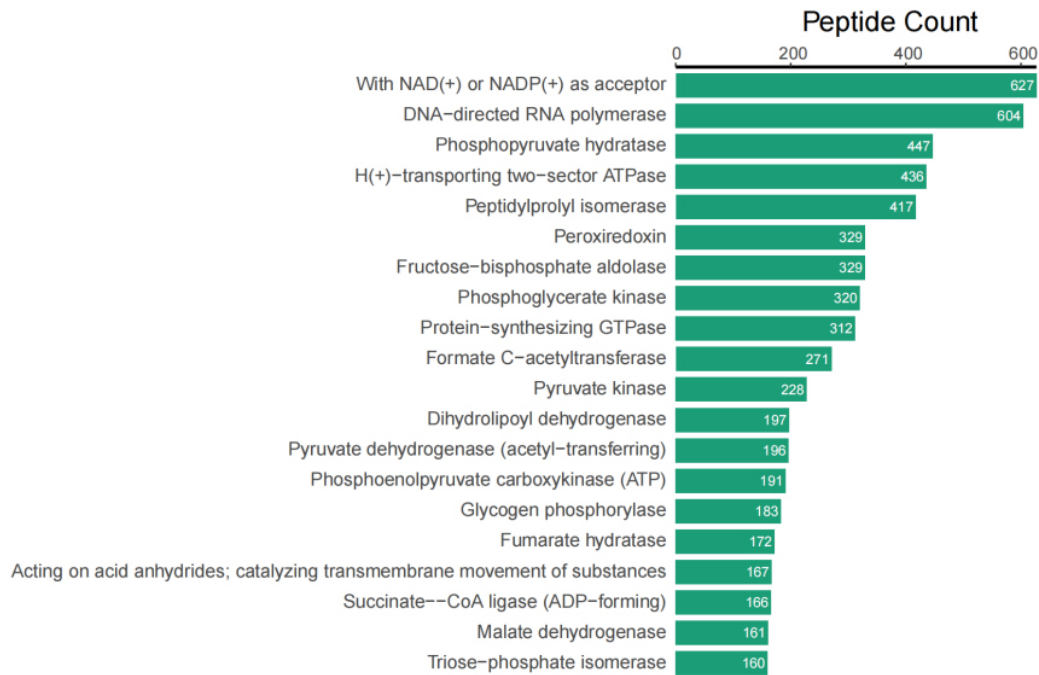


Fig. 3A. Top 20 of peptide counts related to enzymes.

These proteins were assigned to 23 COG categories in five top level classifications, including 1,386 proteins in “Energy production and conversion”, 146 proteins in “Cell cycle control, cell division, chromosome partitioning”, 1,098 proteins in “Amino acid transport and metabolism”, 287 proteins in “Nucleotide transport and metabolism”, 1,335 proteins in “Carbohydrate transport and metabolism”, 259 proteins in “Coenzyme transport and metabolism”, 408 proteins in “Lipid transport and metabolism”, 2,364 proteins in “Translation, ribosomal structure and biogenesis”, 303 proteins in “Transcription”, 184 proteins in “Replication, recombination and repair”, 637 proteins in “Posttranslational modification, protein turnover, chaperones”, 113 proteins in “Cell motility”, 698 proteins in “Posttranslational mod-

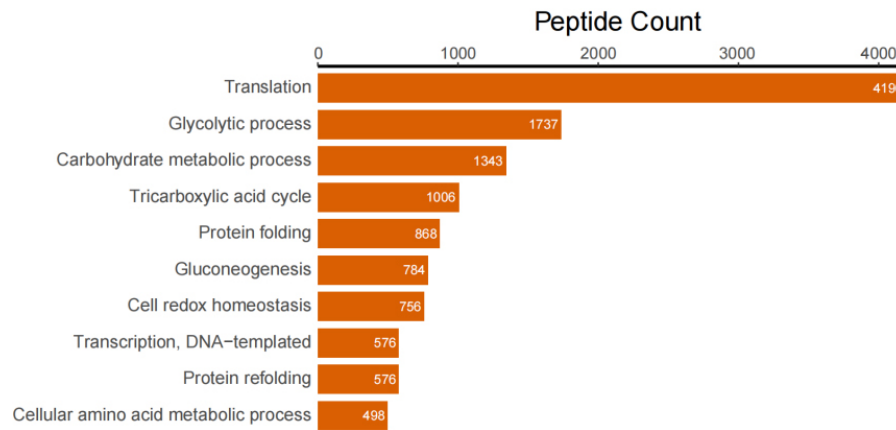


Fig. 3B. Top 10 peptide counts related to GOBP terms.

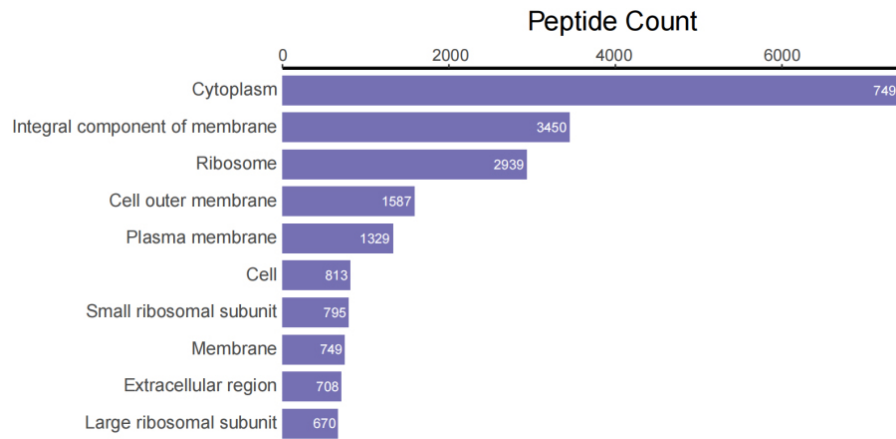


Fig. 3C. Top 10 peptide counts related to GOCC terms.

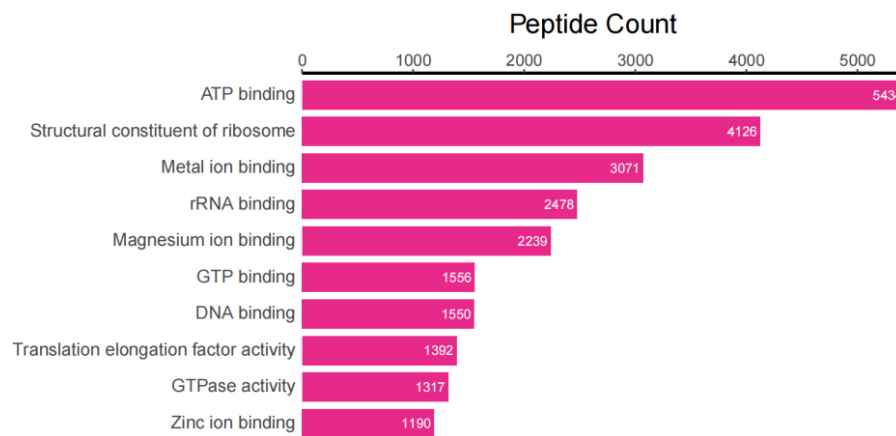


Fig. 3D. Top 10 peptide counts related to GOMF terms.

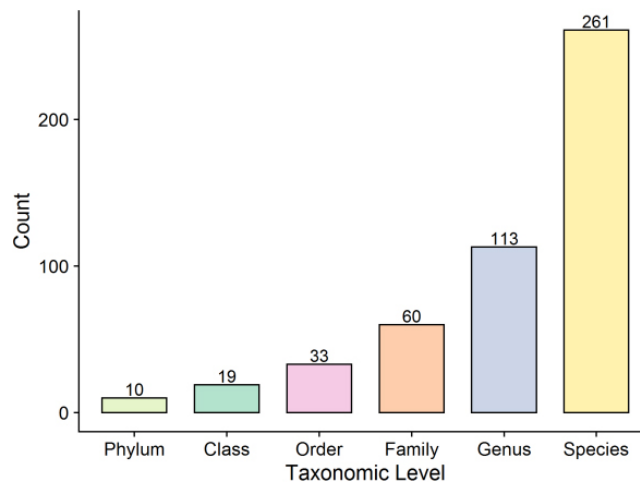


Fig. 4. Protein count of taxonomic levels.

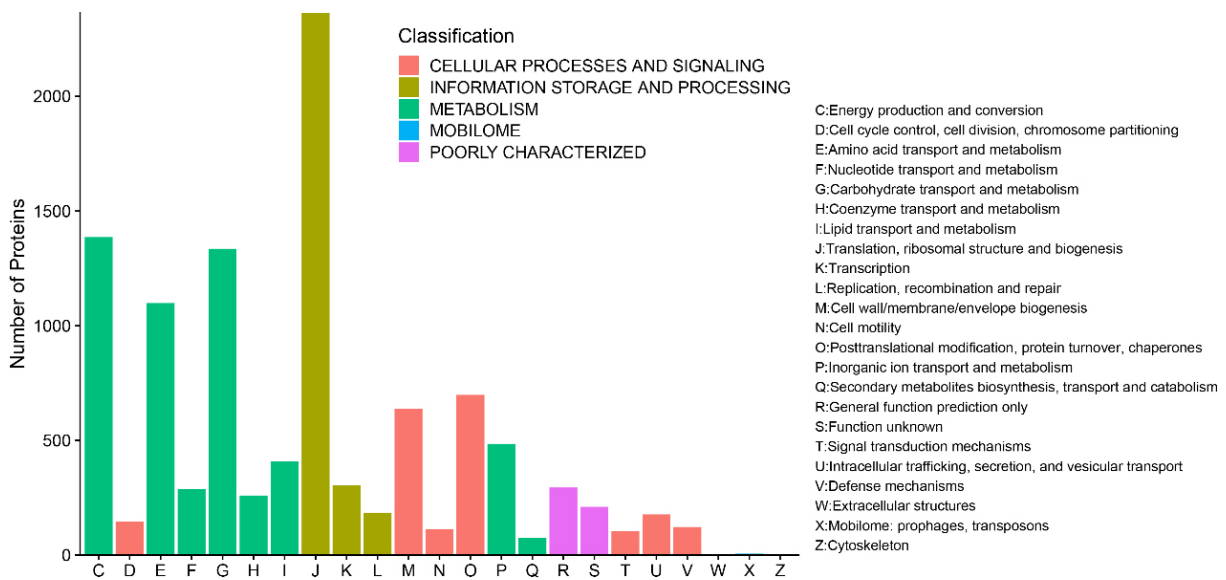


Fig. 5. Bar chart for COG functional classification.

ification, protein turnover, chaperones”, 484 proteins in “Inorganic ion transport and metabolism”, 74 proteins in “Secondary metabolites biosynthesis, transport and catabolism”, 294 proteins in “General function prediction only”, 210 proteins in “Function unknown”, 105 proteins in “Signal transduction mechanisms”, 177 proteins in “Intracellular trafficking, secretion, and vesicular transport”, 122 proteins in “Defense mechanisms”, 2 proteins in “Extracellular structures”, 6 proteins in “Mobilome: prophages, transposons”, and 4 proteins in “Cytoskeleton” (Fig. 5).

At the COG category level, we used the same methods to identify significant differentially abundant categories. Unexpectedly, no significant differentially abundant categories were detected. All p values of the Mann-Whitney U test were greater than 0.05, and the maximum VIP value was less than 2 (R: general function prediction only; VIP = 1.9795).

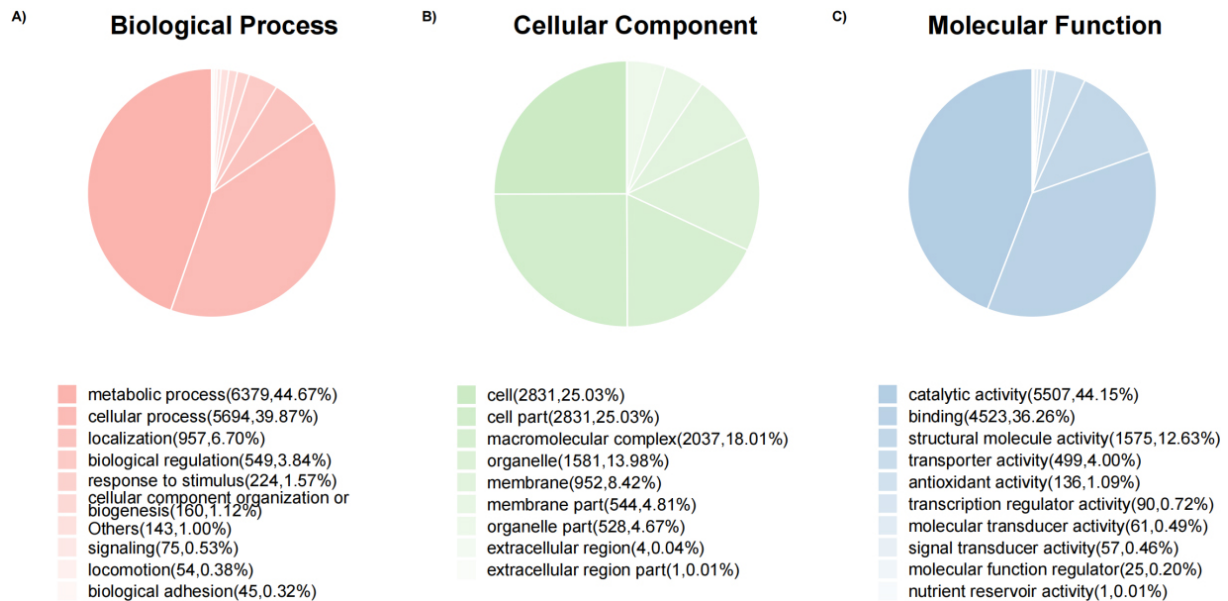


Fig. 6. Pie charts of protein count at the GO level 2 of biological process, cellular component, and molecular function ontology.

### 3.4. Gene ontology functional analysis

Overall, 9194 (80.16%) top identified microbial proteins in general, according to interproscan and internal Perl scripts, these top identified microbial proteins correspond to at least one go term. The number of proteins is counted at the GO level 2 of biological processes, cellular components and molecular functional Ontology (Fig. 6). Then, Fisher's exact test was performed to compare the difference in the number of proteomes between group B and group Z. Based on  $p < 0.05$ , GO terms in group B were significantly richer than those in group Z, including 35 entries in biological process ontology, 2 entries in cell component ontology, and 30 entries in molecular function ontology. GO terms in group Z were significantly richer than those in group B, including 59 entries in biological process, 17 entries in cell component, and 30 entries in molecular function ontology (Fig. 7).

Use internal Perl and R scripts to enumerate the proteins corresponding to the go items of all samples. Fisher's exact test was performed using R to determine important GO items based on the number of proteins in paired samples from the same patient. At  $p < 0.05$ , in at least 12 paired samples, 80 GO terms in group Z (33 terms in biological process ontology, 5 terms in cell component ontology, 42 terms in molecular function ontology) were significantly richer than those in group B. compared with group Z, only 10 GO terms in group B were richer (8 in biological process ontology, 2 in molecular function ontology). Then, we use the negative logarithm 10 to convert the p value and use the heat map generated by R to visualize the data (Fig. 8).

### 3.5. Pathway analysis based on KEGG

A total of 9,039 top identified microbial proteins were annotated in the KEGG database using KOBAS 3.0. These proteins were related to 1,385 nonredundant KO identifiers and assigned to 196 KEGG pathways belonging to 41 KEGG categories of the 6 top classifications (Fig. 9).

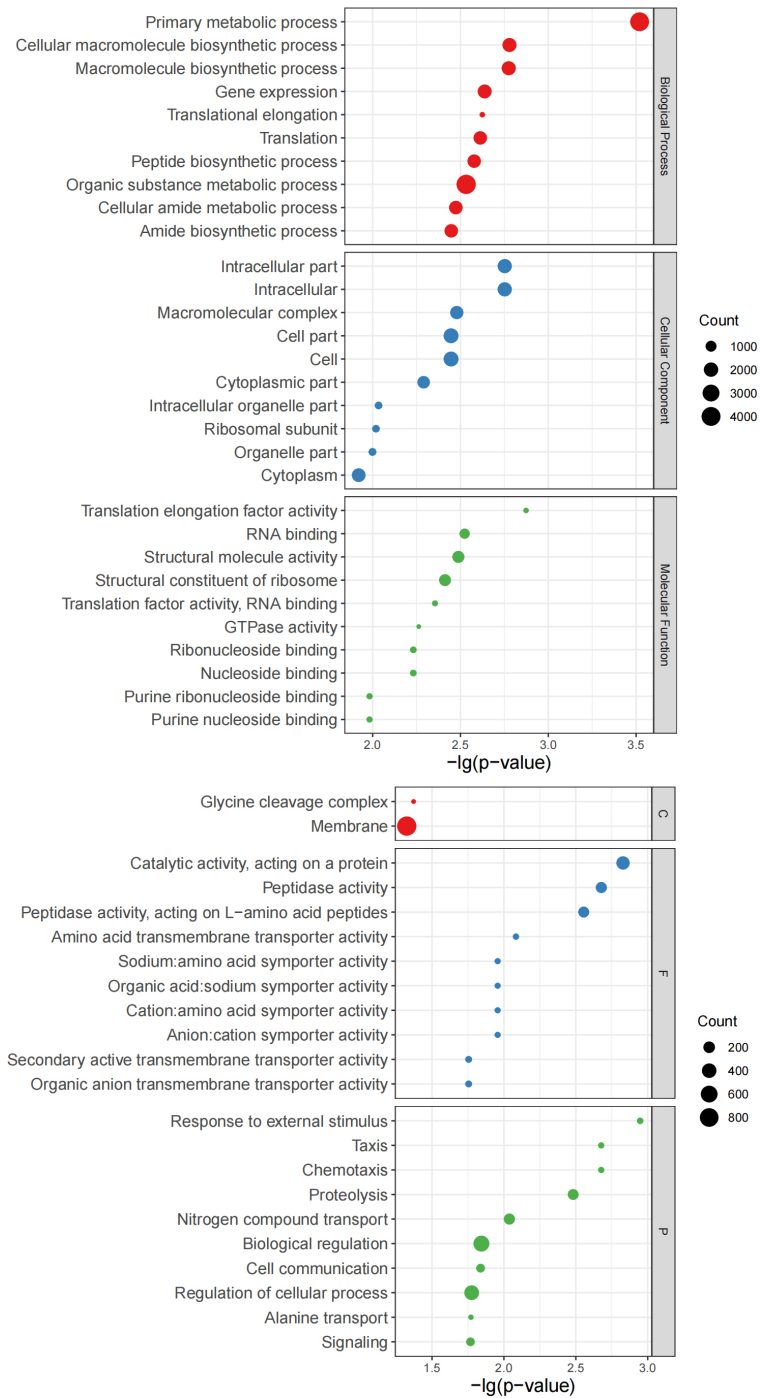


Fig. 7. Bubble charts of top 10 GO terms. Left: Top 10 GO terms of Group B significantly more abundant than those of Group Z. Right: Top 10 GO terms of Group Z significantly more abundant than those of Group B. Y-axis corresponds to significant GO terms, and X-axis corresponds to negative  $\log_{10}$  transformed  $p$  value according to the results of the Fisher's exact test. The dot size corresponds to protein counts.

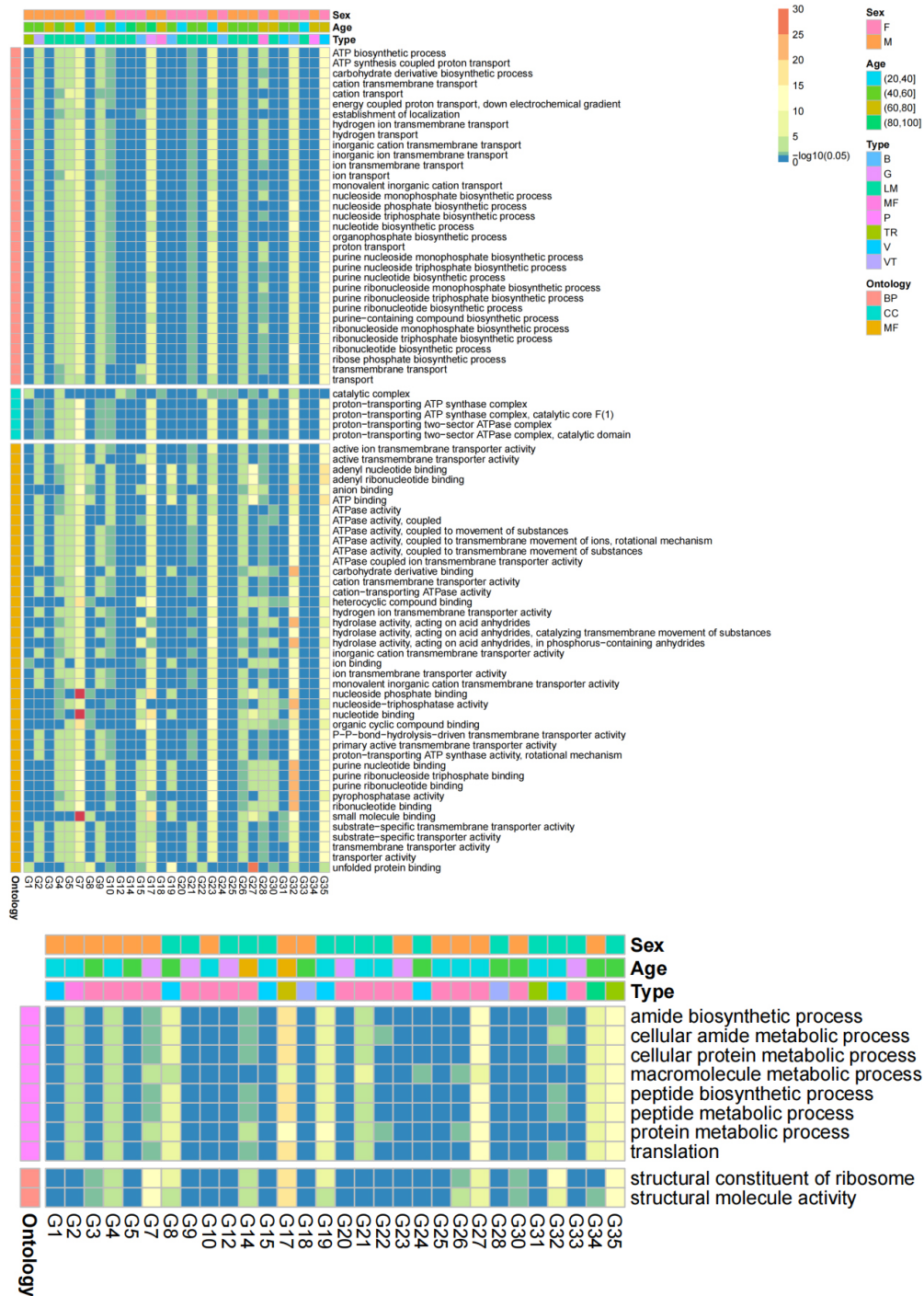


Fig. 8. Heatmaps of transformed p values of significant GO terms in at least 12 sample pairs. A) Significant GO terms of the Z group were more abundant than those of the B group; B) Significant GO terms of the B group were more abundant than those of the Z group.

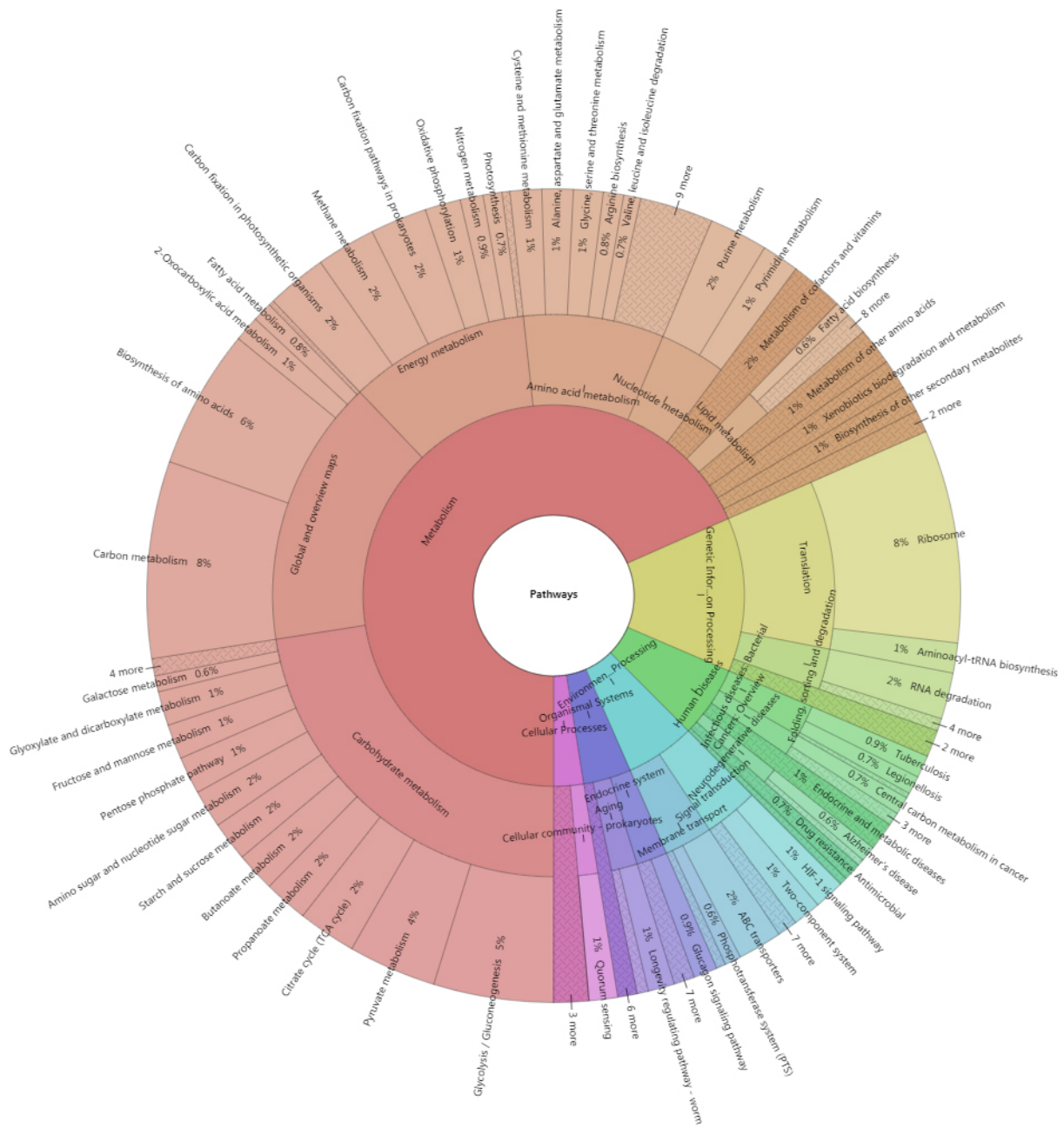


Fig. 9. KRONA plot of proteins corresponding to the KEGG pathways. KRONA plot shows the proportion of proteins assigned to the KEGG pathways from the top levels to specific pathways.

Significantly different pathways with  $p < 0.05$ , according to the binomial test via KOBAS 3.0 based on the protein counts in the pathways, were identified as 8 pathways of Group B more abundant than those in Group Z. In these pathways, the FDR-corrected  $p$  values of the bacterial secretion system (FDR = 0.017) and protein export (FDR = 0.024) were less than 0.05. Moreover, we identified 18 significantly different

Table 2  
Significantly different pathways

Significantly different pathways in Group B vs. Group Z evaluated by statistical methods.

Term	Protein count in Group B	Protein count in Group Z	<i>P</i> value	FDR
Bacterial secretion system	68	32	$1.21 \times 10^{-4}$	$1.70 \times 10^{-2}$
Protein export	61	29	$3.34 \times 10^{-4}$	$2.35 \times 10^{-2}$
Lipopolysaccharide biosynthesis	24	9	$1.14 \times 10^{-3}$	$5.37 \times 10^{-2}$
Aminoacyl-tRNA biosynthesis	209	133	$4.97 \times 10^{-3}$	$1.75 \times 10^{-1}$
Phenylalanine, tyrosine and tryptophan biosynthesis	35	17	$7.35 \times 10^{-3}$	$2.07 \times 10^{-1}$
Porphyrin and chlorophyll metabolism	59	34	$2.09 \times 10^{-2}$	$4.92 \times 10^{-1}$
Bacterial chemotaxis	65	39	$3.28 \times 10^{-2}$	$6.61 \times 10^{-1}$
Phenylalanine metabolism	33	18	$3.77 \times 10^{-2}$	$6.64 \times 10^{-1}$

Significantly different pathways in Group Z vs. Group B evaluated by statistical methods.

Term	Protein count in Group Z	Protein count in Group B	<i>P</i> value	FDR
Glycolysis/Gluconeogenesis	784	885	$1.06 \times 10^{-4}$	$1.63 \times 10^{-3}$
Ribosome	1298	1545	$1.09 \times 10^{-4}$	$5.83 \times 10^{-3}$
Carbon metabolism	1195	1417	$1.29 \times 10^{-4}$	$5.83 \times 10^{-3}$
RNA degradation	321	342	$1.52 \times 10^{-4}$	$5.83 \times 10^{-3}$
Biosynthesis of amino acids	851	996	$3.59 \times 10^{-4}$	$1.08 \times 10^{-2}$
HIF-1 signaling pathway	219	227	$4.20 \times 10^{-4}$	$1.08 \times 10^{-2}$
Methane metabolism	381	422	$6.28 \times 10^{-4}$	$1.38 \times 10^{-2}$
Tuberculosis	165	168	$9.84 \times 10^{-4}$	$1.89 \times 10^{-2}$
Carbon fixation in photosynthetic organisms	399	449	$1.36 \times 10^{-3}$	$2.32 \times 10^{-2}$
Longevity regulating pathway – worm	181	194	$4.67 \times 10^{-3}$	$7.19 \times 10^{-2}$
Alzheimer's disease	113	117	$8.74 \times 10^{-3}$	$1.19 \times 10^{-1}$
Legionellosis	129	136	$9.28 \times 10^{-3}$	$1.19 \times 10^{-1}$
Type I diabetes mellitus	84	85	$1.29 \times 10^{-2}$	$1.48 \times 10^{-1}$
Pyruvate metabolism	531	632	$1.35 \times 10^{-2}$	$1.48 \times 10^{-1}$
Glucagon signaling pathway	159	174	$1.46 \times 10^{-2}$	$1.50 \times 10^{-1}$
Propanoate metabolism	269	312	$2.56 \times 10^{-2}$	$2.47 \times 10^{-1}$
Photosynthesis	128	141	$3.04 \times 10^{-2}$	$2.75 \times 10^{-1}$
Insulin resistance	61	63	$4.11 \times 10^{-2}$	$3.52 \times 10^{-1}$

pathways of Group Z more abundant than those of Group B using the same method. Nine pathways had an FDR < 0.05, including glycolysis/gluconeogenesis (FDR = 0.0016), ribosomes (FDR = 0.0058), carbon metabolism (FDR = 0.0058), RNA degradation (FDR = 0.0058), biosynthesis of amino acids (FDR = 0.0108), HIF-1 signaling pathway (0.0108), methane metabolism (FDR = 0.0138), tuberculosis (FDR = 0.0189), and carbon fixation in photosynthetic organisms (FDR = 0.0232). Moreover, a paired sample test used the same methods to obtain significantly different pathways. A total of 72 pathways with at least one *p* value of paired sample test less than 0.05 were identified in the case of Group B vs. Group Z, and a total of 88 pathways were identified in the case of Group Z vs. Group B. Some pathways were significantly more abundant in Group B than those in Group Z based on the binomial test selection of at least 9 paired sample tests with a *p* value < 0.05, including carbon fixation in photosynthetic organisms (9), HIF-1 signaling pathway (9), ribosome (9), and carbon metabolism (10); carbon fixation in photosynthetic organisms (9), oxidative phosphorylation (9), Alzheimer's disease (10), methane metabolism (10), biosynthesis of amino acids(11), glycolysis/gluconeogenesis (12), HIF-1 signaling pathway (12), photosynthesis (12), longevity regulating pathway – worm (14), tuberculosis (14), and RNA degradation (17) were more abundant in Group Z than the corresponding pathways in Group B. (Table 2).

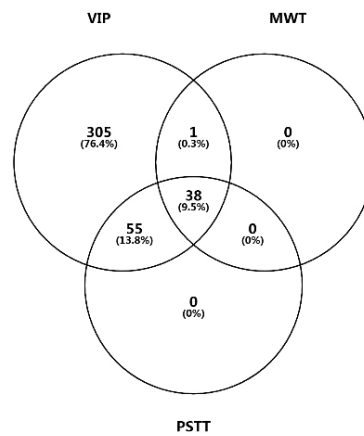


Fig. 10A. Venn diagram for candidate DEPs identified by PLS-DA (VIP), Mann-Whitney U test (MWT), and paired sample T test (PSTT).

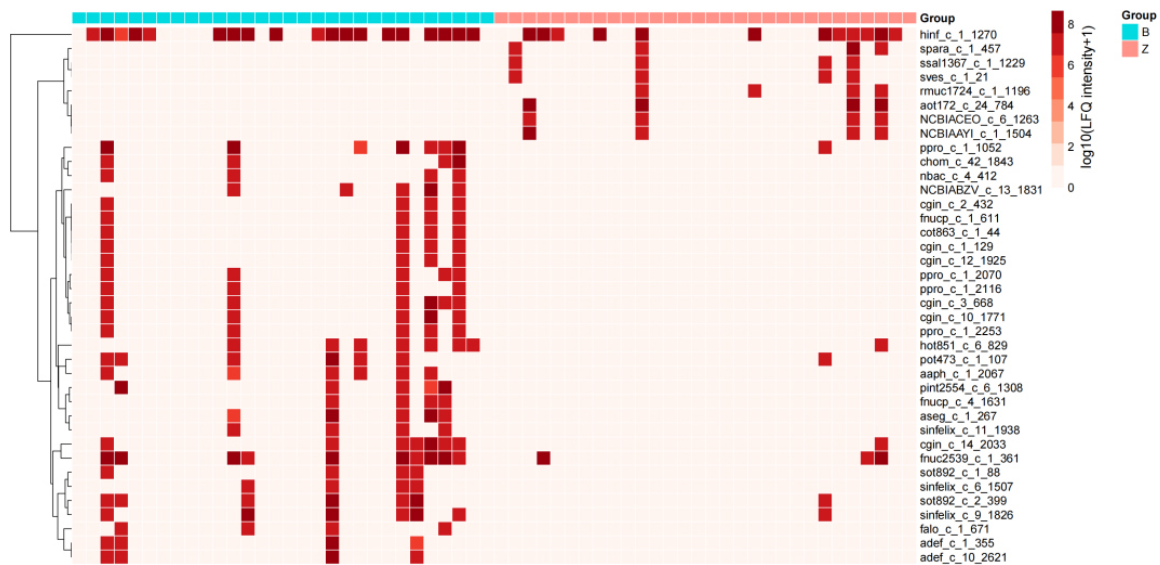


Fig. 10B. Heatmap of DEPs. Row clustering includes Manhattan distance and complete linkage.

### 3.6. Selection of differentially expressed proteins

Log<sub>10</sub>-transformed LFQ intensities were used to identify a total of 39 protein groups as candidate significantly differentially expressed proteins (DEPs) in the B versus Z groups according to the Mann-Whitney U test at a cutoff  $p$  value  $< 0.05$ . Moreover, a total of 93 candidate DEPs were identified using a paired sample T test with a cutoff  $p$  value  $< 0.05$ . Furthermore, missing values were imputed as one thousandth of the minimum values, and PLS-DA was performed. A total of 399 candidate DEPs were assessed based on  $VIP > 2$ . DEPs obtained by the three methods were used to plot a Venn diagram (Fig. 10A), and 38 common DEPs were finally identified and illustrated on a heatmap generated by the pheatmap package (Fig. 10B). Receiver operating characteristic (ROC) analysis was performed on 38 common candidate DEPs using the MetaboAnalystR package.

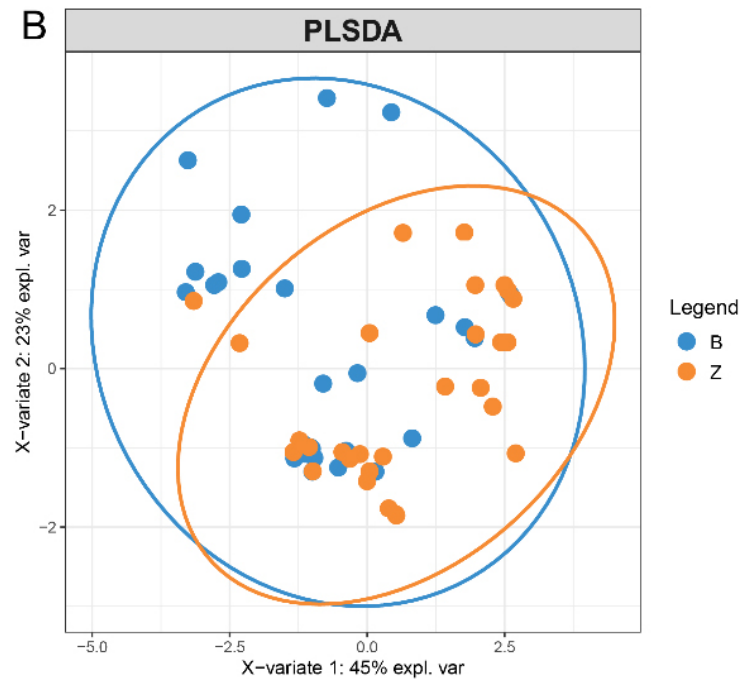


Fig. 11. PCA score plot of proteins quantified in  $\geq 50\%$  of the samples. B) PLS-DA score plot of proteins quantified in  $\geq 50\%$  of the samples.

### 3.7. Multidimensional variable analysis

We selected proteins quantified in  $\geq 50\%$  of the samples for principal component analysis (PCA) and partial least squares discriminant analysis (PLS-DA). A total of 10 proteins were selected. PCA and PLS-DA were performed using these proteins by the mixOmics package in R. (Fig. 11).

### 3.8. Mass spectrometry analysis of PRM validation candidate peptides and proteins

The results of PRM indicated that the 22Z and 22B samples were unsuitable for analysis. Therefore, these two samples were removed from the analysis. Finally, the results of 56 samples from 28 patients were used to perform differentially expressed peptides and protein analysis. We used R (version 3.5.1) software to perform paired sample T test for the selection of differentially expressed peptides and proteins, respectively.

The results of the analysis of proteins identified 10 and 11 candidate differentially expressed proteins according to the paired sample T test with  $p < 0.05$ , respectively. The combination of candidate differentially expressed proteins included 2 proteins (hinf\_c\_1\_1270 and fnuc2539\_c\_1\_361) that were determined to be candidate differentially expressed proteins according to metaproteomics analysis [17] (Table 3), and the intersection included 5 proteins.

## 4. Discussion

Consistency of the results obtained by three different approaches used in the present study was high, and there were no significant differences between these results, indicating that the experiment had very

Table 3  
Candidate differentially expressed proteins confirmed by the paired sample T test

Protein ID	<i>P</i> value of paired sample T test	Fold change
cgra1653_c_8_2197	$1.25 \times 10^{-1}$	1.84
chom_c_55_2089	$9.10 \times 10^{-3}$	3.50
cot326_c_18_1175	$3.32 \times 10^{-2}$	3.71
cot338_c_14_1730	$6.62 \times 10^{-2}$	2.73
cper_c_3_388	$2.20 \times 10^{-1}$	31.33
esak_c_1_3563	$4.18 \times 10^{-2}$	2.50
fnuc2539_c_1_361	$4.63 \times 10^{-2}$	8.51
fnuc420_c_16_2114	$7.68 \times 10^{-2}$	1.98
fnucp_c_1_589	$5.86 \times 10^{-3}$	3.74
hinf_c_1_1270	$1.04 \times 10^{-2}$	3.29
NCBIACEO_c_3_753	$4.56 \times 10^{-2}$	2.64
NCBIACEO_c_3_844	$4.47 \times 10^{-1}$	2.15
NCBIACEO_c_7_1474	$3.12 \times 10^{-2}$	2.22
nsic_c_12_1571	$4.43 \times 10^{-3}$	5.20
pend_c_10_1352	$2.64 \times 10^{-2}$	2.84
rmuc_c_1_178	$4.74 \times 10^{-2}$	2.31

good repeatability, and the results were relatively stable. Statistical evaluation identified upregulated and downregulated proteins to illustrate that the number of DEPs was the largest in the B group versus those in the Z group. The heatmap demonstrated that variation in DEP expression in the B group was greater than that in the Z group.

COG functional analysis illustrated that “energy production and conversion” was significantly enriched in the B group. In this category, the number of proteins downregulated in the B group versus those in the Z group was higher than the number of the corresponding upregulated proteins. Thus, energy production and conversion of bacteria was weaker in the B group. Quantitative proteomics analysis performed by Suriyanarayanan demonstrated that metabolic activity of strong biofilm-forming bacteria was weaker than that of weak biofilm-forming bacteria [16]. The authors suggested that lower metabolic activity may promote adhesion instead of dispersal to protect the bacteria from harmful conditions.

Moreover, “proton transport”, “hydrogen transport”, and “hydrogen ion transmembrane transport” were the top 3 enriched GO categories of the B group versus the Z group. The major downregulated DEPs were related to F-type ATP synthase, and the major upregulated DEPs were related to V-type ATP synthase. Significant downregulation of F1F0 ATP synthase subunits encoded by *atpABCDEF*G suggested that proton motive force-driven ATP synthesis was weakened. Upregulation of V-ATP synthase subunits encoded by *atpABD* implied that ATP-dependent proton pumps were enhanced, which induced acidification of luminal environments [17]. This process may be due to an external environment, which forced the bacteria to pump hydrogen ions to adjust the pH of their microenvironment to maintain acid-base balance. As a result, the activity of hydrogen-dependent ATP synthesis was decreased, and the proteins related to F-type ATP synthase were downregulated. Additionally, a protein related to H<sup>+</sup>-transporting two-sector ATPase encoded by *EFNG\_00349* was significantly increased in both groups in accordance with this phenomenon.

ATP-binding cassette (ABC) transporters represent another category of numerous proteins undergoing significant changes. Two types of ABC transporters with different functions were upregulated and downregulated. Upregulated proteins included ATP-binding proteins related to ATPase activity in the B group versus Z group. These proteins may be related to ATP-dependent proton pump activity mediated by V-ATP synthase, as described above. Downregulated proteins included permease proteins that were mainly

responsible for transmembrane transport in the B group versus Z group. Zhu et al. [18] reported that the G\_1771 gene of *Listeria monocytogenes*, which encodes a putative ABC transporter permease, is involved in negative regulation of biofilm formation. The authors analyzed an *lm.G\_1771* gene deletant strain by phenotypic, proteomic, and genomic methods and demonstrated that certain genes are downregulated, including *dltABCD* operons involved in negative regulation of biofilm formation [18]. *DltABCD* plays a role in the binding of positively charged D-alanine residues to lipoteichoic acid of the bacterial membrane. Downregulation of these genes may lead to a negative charge on the bacterial surface. In the present study, permease proteins of ABC transporters, proteins encoded by *dltC*, and alanine racemase involved in D-alanine biosynthesis all decreased. A decrease in permease ABC transporters suggested a stronger biofilm-forming ability. Downregulation of the D-alanine carrier protein encoded by *dltC* [19] and alanine racemase reduces the amount of D-alanine bound to LTA on the bacterial surface, which leads to a negative charge on the bacterial surface to resist an increase in  $\text{OH}^-$  concentration in the external environment.

Additionally, the phosphotransferase system (PTS) was another category of proteins significantly altered in the present study. PTS system mannose/fructose/sorbose family IID component, PTS mannose transporter subunit IID, PTS system mannose/fructose/N-acetylgalactosamine-transporter subunit IIB, and PTS system lactose/cellobiose specific IIA subunit were downregulated in the B group, and PTS system cellobiose-specific IIA component was upregulated. PTS plays an important role in the uptake and phosphorylation of sugars. All PTSs consist of two cytoplasmic phosphotransferase proteins and the sugar-specific enzyme II complex. The latter complex consists of the IIA, IIB, and IIC or IICIID subunits [20]. The results of the present study suggested downregulation of the mannose/fructose/sorbose/lactose metabolism pathway. PTS participates in important interactions that regulate bacterial adaptation to stressful environments and antibiotic resistance. Peng et al. [21] demonstrated that intact PTS promotes the adaptation of bacteria to stressful conditions by enhancing their resistance to hydrogen peroxide and acid, production of more harmful substances, such as SOD, survival in macrophages, and regulation of antioxidant and catabolite genes. Wei et al. [22] demonstrated that PTS mediates resistance to multiple drugs by regulating *potA* and/or *OG1RF\_10526* to enhance resistance to nisin, repressing biosynthesis of ribosomes to improve sensitivity to gentamycin and increasing sensitivity to daptomycin. This regulation suggests that PTS may be a direction that should be explored.

In the present study, L-serine dehydratase-related proteins were greatly reduced in the B group. An iron-sulfur cluster-binding protein encoded by *WO5\_01154* was also significantly downregulated since L-serine dehydratases are iron-sulfur proteins [23]. This binding protein may participate in the catalysis of dehydratase. Lindenstrauss et al. [24] demonstrated that the alpha subunit of L-serine dehydratase is anaerobically induced in the *OG1RF* strain. L-Serine dehydratase participates in the degradation of L-serine to ammonium ( $\text{NH}_4^+$ ) and pyruvate. Downregulation of this protein indicates a decrease in the production of  $\text{NH}_4^+$  and pyruvate. The former changes can increase the pH value, and pyruvate is a key intersection of many metabolic pathway networks. As a result, both activities may be negatively affected in the B group, which is consistent with an increase in L-serine consumption observed by Großholz et al. [25], who used SWATH-MS to monitor cellular changes in bacteria under acidic conditions.

A protein encoded by *esp* was downregulated in the B group. There are many contradictory studies on the relationships between *esp* and biofilm formation. Some authors suggested that *esp* is related to formation and degree of the biofilm [26–28], and other authors suggested that *esp* is irrelevant to biofilm [29–32]. In the present study, a trend in transcription was consistent with a trend in protein expression (Fig. 10A and B). A protein encoded by *seal* was upregulated in the B group; The protein is located on the surface of donor bacterial cells, and its main function is to reduce the ineffective binding frequency of sexual pheromones between donor strains [33].

Yan et al. [34] detected the up regulation of SEA1 protein in low-level linezolid resistant strains of *E faecalis*.

A universal stress protein encoded by EFNG\_00797 and the chaperone protein DnaK were upregulated in the B group. The chaperone protein dnaK is considered a stress protein, folding newly synthesized proteins [35].

qPCR and PRM were used to verify the TMT in the present study. The results of qPCR are somewhat different from the data of TMT, and consistency of the PRM data is ideal. These differences may be due to the fact that transcript mRNA levels correspond to only 29–55% of the protein levels in prokaryotes [36], especially in the presence of perturbation-induced changes. PRM is an ion monitoring technology based on high-resolution and high-precision mass spectrometry. The principle of PRM technology is similar to that of SRM/MRM; however, PRM is more commonly used for absolute quantification of proteins and peptides in the development of analytical methods [37–39]. The results of TMT and PRM obtained in the present study are in good agreement, indicating that the results of TMT are reliable.

## 5. Conclusion

Bacterial dysbiosis was observed in the samples of OSCC surface lesions in the present study, with considerable changes in bacterial composition and protein functions compared to those in the control samples. In particular, a group of proteins involved in energy production and conversion, proton transport, hydrogen transport and hydrogen ion transmembrane transport, ATP-binding cassette (ABC) transporter, PTS system, and L-serine dehydratase were significantly enriched in OSCC samples. In addition, we found that some proteins related to actinomycetes and *Clostridium* are highly involved in oral squamous cell carcinoma, which may have good diagnostic ability. The microbiota in oral squamous cell carcinoma is considered to be a synergistic pathogenic factor. From our research results, it is difficult to determine whether dysbacteriosis will change the local microenvironment, so that bacteria suitable for the tumor microenvironment thrive, and then cause cancer. More investigation is still needed. The present study revealed considerable changes in bacterial protein expression in OSCC. These findings provide additional information about an association between the expression of oral bacterial proteins and oral cancer.

## Conflict of interest

The authors declare that they have no conflict of interest.

## Author contributions

WJ, YZ and SR designed the project and wrote the manuscript. ZS supervised the experiments. WXC and ZYH performed the experiments and analyzed the data. All authors read and revised the manuscript.

## Funding

The study was supported by the Shanghai Natural Science Foundation of China (Contract grant number: 18zr1422300); Innovative research team of high-level local universities in Shanghai (SSMU-ZDCX20180901); Fundamental research program funding of Ninth People's Hospital affiliated with

Shanghai Jiao Tong University School of Medicine (JYZZ139); Shanghai Science & Technology Development Foundation (HY202211TUE03); Natural Science Foundation of Tibet Autonomous Region (XZ2019ZR-ZY43(Z)); and the Research Discipline Fund (No. KQYJXK2020) from Ninth People's Hospital, Shanghai Jiao Tong University School of Medicine, and College of Stomatology, Shanghai Jiao Tong University.

## Acknowledgments

The authors thank Shanghai Shengzi Biotechnology Co., Ltd for their effort on LS/MS experiments.

## References

- [1] Chen AY, Myers JN. Cancer of the oral cavity. *Dis Mon.* 2001; 47: 275-361. doi: 10.1067/mcd.2001.109374.
- [2] Flach GB, Verdonck-de Leeuw IM, Witte BI, Klop WM, van Es RJ, Schepman KP, et al. Patients' perspective on the impact of sentinel node biopsy in oral cancer treatment. *Oral Surg Oral Med Oral Pathol Oral Radiol.* 2016; 122: 279-86. doi: 10.1016/j.oooo.2016.03.014.
- [3] Dediol E, Sabol I, Virag M, Grce M, Muller D, Manojlović S. HPV prevalence and p16INKa overexpression in non-smoking non-drinking oral cavity cancer patients. *Oral Dis.* 2016; 22: 517-22. doi: 10.1111/odi.12476.
- [4] Pollard J. Bacteria, inflammation and cancer. *Nat Rev Immunol.* 2015; 15: 528. doi: 10.1038/nri3899.
- [5] Bultman SJ. Emerging roles of the microbiome in cancer. *Carcinogenesis.* 2014; 35: 249-55. doi: 10.1093/carcin/bgt392.
- [6] Nagy KN, Sonkodi I, Szöke I, Nagy E, Newman HN. The microflora associated with human oral carcinomas. *Oral Oncol.* 1998; 34: 304-8. doi: 10.1016/S1368-8375(98)80012-2.
- [7] Hooper SJ, Crean SJ, Lewis MA, Spratt DA, Wade WG, Wilson MJ. Viable bacteria present within oral squamous cell carcinoma tissue. *J Clin Microbiol.* 2006; 44: 1719-25. doi: 10.1128/jcm.44.5.1719-1725.2006.
- [8] Hooper SJ, Crean SJ, Fardy MJ, Lewis MAO, Spratt DA, Wade WG, et al. A molecular analysis of the bacteria present within oral squamous cell carcinoma. *J Med Microbiol.* 2007; 56: 1651-9. doi: 10.1099/jmm.0.46918-0.
- [9] Pushalkar S, Ji X, Li Y, Estilo C, Yegnanarayana R, Singh B, et al. Comparison of oral microbiota in tumor and non-tumor tissues of patients with oral squamous cell carcinoma. *BMC Microbiol.* 2012; 12: 144. doi: 10.1186/1471-2180-12-144.
- [10] Bebek G, Bennett KL, Funchain P, Campbell R, Seth R, Scharpf J, et al. Microbiomic subprofiles and MDR1 promoter methylation in head and neck squamous cell carcinoma. *Hum Mol Genet.* 2012; 21: 1557-65. doi: 10.1093/hmg/ddr593.
- [11] Wang H, Funchain P, Bebek G, Altemus J, Zhang H, Niazi F, et al. Microbiomic differences in tumor and paired-normal tissue in head and neck squamous cell carcinomas. *Genome Med.* 2017; 9: 14. doi: 10.1186/s13073-017-0405-5.
- [12] Pushalkar S, Mane SP, Ji X, Li Y, Evans C, Crasta OR, et al. Microbial diversity in saliva of oral squamous cell carcinoma. *FEMS Immunol Med Microbiol.* 2011; 61: 269-77. doi: 10.1111/j.1574-695X.2010.00773.x.
- [13] Guerrero-Preston R, Godoy-Vitorino F, Jedlicka A, Rodríguez-Hilario A, González H, Bondy J, et al. 16S rRNA amplicon sequencing identifies microbiota associated with oral cancer, human papilloma virus infection and surgical treatment. *Oncotarget.* 2016; 7: 51320-34. doi: 10.18632/oncotarget.9710.
- [14] Al-Hebshi NN, Nasher AT, Idris AM, Chen T. Robust species taxonomy assignment algorithm for 16S rRNA NGS reads: application to oral carcinoma samples. *J Oral Microbiol.* 2015; 7: 28934. doi: 10.3402/jom.v7.28934.
- [15] Al-Hebshi NN, Nasher AT, Maryoud MY, Homeida HE, Chen T, Idris AM, et al. Inflammatory bacteriome featuring *Fusobacterium nucleatum* and *Pseudomonas aeruginosa* identified in association with oral squamous cell carcinoma. *Sci Rep.* 2017; 7: 1834. doi: 10.1038/s41598-017-02079-3.
- [16] Suriyanarayanan T, Qingsong L, Kwang LT, Mun LY, Truong T, Seneviratne CJ. Quantitative proteomics of strong and weak biofilm formers of *Enterococcus faecalis* reveals novel regulators of biofilm formation. *Mol Cell Proteomics.* 2018; 17: 643-54. doi: 10.1074/mcp.RA117.000461.
- [17] Kane PM. The where, when, and how of organelle acidification by the yeast vacuolar H<sup>+</sup>-ATPase. *Microbiol Mol Biol Rev.* 2006; 70: 177-91. doi: 10.1128/mmb.70.1.177-191.2006.
- [18] Zhu X, Liu W, Lametsch R, Aarestrup F, Shi C, She Q, et al. Phenotypic, proteomic, and genomic characterization of a putative ABC-transporter permease involved in *Listeria monocytogenes* biofilm formation. *Foodborne Pathog Dis.* 2011; 8: 495-501. doi: 10.1089/fpd.2010.0697.
- [19] Fabretti F, Theilacker C, Baldassarri L, Kaczynski Z, Kropec A, Holst O, et al. Alanine esters of enterococcal lipoteichoic acid play a role in biofilm formation and resistance to antimicrobial peptides. *Infect Immun.* 2006; 74: 4164-71. doi: 10.1128/iai.00111-06.

- [20] Jeckelmann JM, Erni B. The mannose phosphotransferase system (Man-PTS) – Mannose transporter and receptor for bacteriocins and bacteriophages. *Biochim Biophys Acta Biomembr.* 2020; 1862: 183412. doi: 10.1016/j.bbmem.2020.183412.
- [21] Peng Z, Ehrmann MA, Waldhuber A, Niemeyer C, Miethke T, Frick JS, et al. Phosphotransferase systems in *Enterococcus faecalis* OG1RF enhance anti-stress capacity *in vitro* and *in vivo*. *Res Microbiol.* 2017; 168: 558-66. doi: 10.1016/j.resmic.2017.03.003.
- [22] Wei L, Li M, Xia F, Wang J, Ran S, Huang Z, et al. Phosphate transport system mediates the resistance of *Enterococcus faecalis* to multidrug. *Microbiol Res.* 2021; 249: 126772. doi: 10.1016/j.micres.2021.126772.
- [23] Cicchillo RM, Baker MA, Schnitzer EJ, Newman EB, Krebs C, Booker SJ. *Escherichia coli* L-serine deaminase requires a [4Fe-4S] cluster in catalysis. *J Biol Chem.* 2004; 279: 32418-25. doi: 10.1074/jbc.M404381200.
- [24] Lindenstrauss AG, Behr J, Ehrmann MA, Haller D, Vogel RF. Identification of fitness determinants in *Enterococcus faecalis* by differential proteomics. *Arch Microbiol.* 2013; 195: 121-30. doi: 10.1007/s00203-012-0857-3.
- [25] Großholz R, Koh CC, Veith N, Fiedler T, Strauss M, Olivier B, et al. Integrating highly quantitative proteomics and genome-scale metabolic modeling to study pH adaptation in the human pathogen *Enterococcus faecalis*. *NPJ Syst Biol Appl.* 2016; 2: 16017. doi: 10.1038/npjbsa.2016.17.
- [26] Tendolkar PM, Baghdayan AS, Gilmore MS, Shankar N. Enterococcal surface protein, Esp, enhances biofilm formation by *Enterococcus faecalis*. *Infect Immun.* 2004; 72: 6032-9. doi: 10.1128/iai.72.10.6032-6039.2004.
- [27] Tendolkar PM, Baghdayan AS, Shankar N. The N-terminal domain of enterococcal surface protein, Esp, is sufficient for Esp-mediated biofilm enhancement in *Enterococcus faecalis*. *J Bacteriol.* 2005; 187: 6213-22. doi: 10.1128/jb.187.17.6213-6222.2005.
- [28] Toledo-Arana A, Valle J, Solano C, Arrizubieta MJ, Cucarella C, Lamata M, et al. The enterococcal surface protein, Esp, is involved in *Enterococcus faecalis* biofilm formation. *Appl Environ Microbiol.* 2001; 67: 4538-45. doi: 10.1128/aem.67.10.4538-4545.2001.
- [29] Dworniczek E, Wojciech Ł, Sobieszczkańska B, Seniuk A. Virulence of *Enterococcus* isolates collected in Lower Silesia (Poland). *Scand J Infect Dis.* 2005; 37: 630-6. doi: 10.1080/00365540510031421.
- [30] Kristich CJ, Li YH, Cvitkovitch DG, Dunny GM. Esp-independent biofilm formation by *Enterococcus faecalis*. *J Bacteriol.* 2004; 186: 154-63. doi: 10.1128/jb.186.1.154-163.2004.
- [31] Mohamed JA, Murray BE. Lack of correlation of gelatinase production and biofilm formation in a large collection of *Enterococcus faecalis* isolates. *J Clin Microbiol.* 2005; 43: 5405-7. doi: 10.1128/jcm.43.10.5405-5407.2005.
- [32] Ramadhan AA, Hegedus E. Biofilm formation and esp gene carriage in enterococci. *J Clin Pathol.* 2005; 58: 685-6. doi: 10.1136/jcp.2004.024109.
- [33] Weidlich G, Wirth R, Galli D. Sex pheromone plasmid pAD1-encoded surface exclusion protein of *Enterococcus faecalis*. *Mol Gen Genet.* 1992; 233: 161-8. doi: 10.1007/bf00587575.
- [34] Yan J, Xia Y, Yang M, Zou J, Chen Y, Zhang D, et al. Quantitative proteomics analysis of membrane proteins in *Enterococcus faecalis* with low-level linezolid-resistance. *Front Microbiol.* 2018; 9: 1698. doi: 10.3389/fmicb.2018.01698.
- [35] Pfanner N. Who chaperones nascent chains in bacteria? *Curr Biol.* 1999; 9: R720-4. doi: 10.1016/s0960-9822(99)80467-9.
- [36] Taniguchi Y, Choi PJ, Li GW, Chen H, Babu M, Hearn J, et al. Quantifying *E. coli* proteome and transcriptome with single-molecule sensitivity in single cells. *Science.* 2010; 329: 533-8. doi: 10.1126/science.1188308.
- [37] Bourmaud A, Gallien S, Domon B. Parallel reaction monitoring using quadrupole-Orbitrap mass spectrometer: principle and applications. *Proteomics.* 2016; 16: 2146-59. doi: 10.1002/pmic.201500543.
- [38] Peterson AC, Russell JD, Bailey DJ, Westphall MS, Coon JJ. Parallel reaction monitoring for high resolution and high mass accuracy quantitative, targeted proteomics. *Mol Cell Proteomics.* 2012; 11: 1475-88. doi: 10.1074/mcp.O112.020131.
- [39] Mesuere B, Debyser G, Aerts M, Devreese B, Vandamme P, Dawyndt P. The Unipept metaproteomics analysis pipeline. *Proteomics.* 2015; 15: 1437-42. doi: 10.1002/pmic.201400361.